

Experimental Study of the Effect of Concrete Strength on Shear Wall Behavior

Hideaki Saito, Rikiro Kikuchi
 Tokyo Electric Power Company, Tokyo, Japan
 M. Kanechika, Kimio Okamoto
 Kajima Corporation, Tokyo, Japan

INTRODUCTION

This study confirmed experimentally the effects of reduced wall thickness on the structural behavior of shear walls using higher strength concrete than usual. The consequent reduction of building weight is expected to contribute to the advancement of the design and construction of nuclear power plants. Recently such higher strength concrete has been used in nuclear power plants in Japan.

OUTLINE OF THE TEST RESULTS

A total of fifteen specimens of shear walls were tested to examine the shearing behavior using three different loading types. Higher strength concrete, $F_c=360\text{kgf/cm}^2$ {35MPa}, was compared with conventional concrete of $F_c=240\text{kgf/cm}^2$ {23MPa}. Wall thickness was reduced in inverse proportion to the square root of the concrete strength value, so the wall thickness of the specimens with strength $F_c=360\text{kgf/cm}^2$ was fixed at 80% of the specimens with strength $F_c=240\text{kgf/cm}^2$. The same loading schedule was used for the three different types of the tests in which cyclic lateral loadings were applied alternately under the constant axial loading.

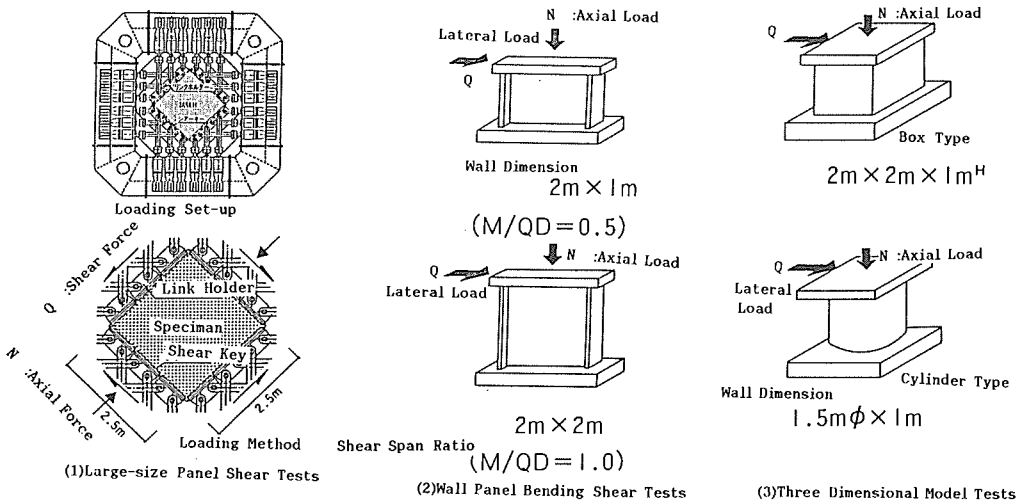


Fig. 1 Kinds of Tests

(1) LARGE-SIZE PANEL SHEAR TEST

The object of this test was to grasp the structural behavior of a shear wall element under pure shearing force, and tests were conducted as a shearing test using the large panel loading system. Table 1 shows a list of concrete

specimen specifications. Fig.2 shows details of the panel test and test specimen. Two specimens were made from concrete of different strength, both being 2.5m square. The thickness of the $F_c=360\text{kgf/cm}^2$ specimen was 13.4cm and that of the $F_c=240\text{kgf/cm}^2$ specimen was 16.7cm. Reinforcing bars, diameter 10mm, were arranged 75 mm mesh in two layers spaced 97mm apart for both directions. Though the amount of bars used was equal for each specimen, the web reinforcement ratios differed between specimens due to the difference in wall thicknesses. Table 2 showed the mechanical properties of the concrete specimens. Using a large panel loading system, mounted 24 actuators, combined loads of one-direction constant compressive axial load ($\sigma_0=20\text{kgf/cm}^2$ (2.0MPa)) and an in-plane shear force were applied as illustrated in Fig.1.

Test results are shown in Table 3 and Fig.3. The initial rigidity of the specimens did not differ, and test results were twice the calculated values. The initial shear cracking load was higher for the L-2 specimen than the L-1 specimen, and after the appearance of cracks degree of rigidity declined gradually. The cyclic hysteresis loop was stable shaped due to the action of the constant axial force and the slipping was not observed. Maximum shear capacities in the test were less than the calculated values because the periphery of the specimens suffered local cracks due to shear compressive force.

Table 1 List of Specimen

Specimen	Concrete Strength F_c (kgf/cm ²)	Wall Thickness t (cm)	Web Reinforcement Ratio P_w (%)	Compressive Axial Stress σ_0 (kgf/cm ²)
L-1	240	16.7	1.14 (D10@75 \times)	20.0
L-2	360	13.4	1.41 (D10@75 \times)	20.0

$\frac{1}{2}$ 2 Layers

Table 2 Mechanical Properties of Concrete

Specimen	Compressive Strength σ_B (kgf/cm ²)	Young's Modulus E_s (kgf/cm ²)	Maximum Strain ϵ_s (%)	Tensile Strength σ_T (kgf/cm ²)
L-1	263	2.26×10^5	0.245	26.6
L-2	347	2.44×10^5	0.242	24.1

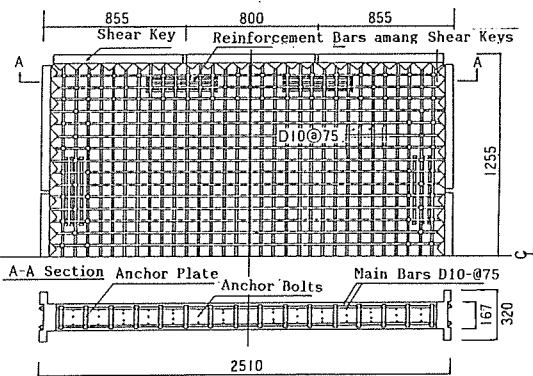


Fig. 2 Details of Panel Specimen

(2) I-SHAPED WALL PANEL BENDING SHEAR TESTS

The aim of this test was to confirm the applicability of values estimated by conventional formulas regarding ultimate load carrying capacities, etc., so the authors performed a bending shear test using I-shaped wall panels. The nine specimens were constructed with the following parameters : concrete strength, ratio of web reinforcement, shear span ratio, and axial load. The specimen using the $F_c=240\text{kgf/cm}^2$ strength concrete had a wall thickness of 15cm, and the specimens using $F_c=360\text{kgf/cm}^2$ and $F_c=420\text{kgf/cm}^2$ (41MPa) strength concrete had wall thicknesses of 12cm. Table 4 shows the types of specimens, and Fig.4 shows representative details of the bending shear tests. Fig.5 shows the

Table 3 Comparison of Tests Results and Calculated Value (1kgf/cm²=0.098MPa)

Specimen	L-1			L-2		
	T.V	C.V	T.V/C.V	T.V	C.V	T.V/C.V
Elastic Shear Rigidity $K_0 (\times 10^3 \text{ t/cm})$	2.26	1.03	2.19	2.76	1.19	2.32
Shear Cracks Stress $\tau_{cr} (\text{kgf/cm}^2)$	24.0	24.2	0.99	28.0	26.8	1.04
Shear Yielding Stress $\tau_y (\text{kgf/cm}^2)$	49.0 ^{*1}	53.2	0.92	52.0 ^{*1}	63.4	0.82
Ultimate Shear Capacity $\tau_u (\text{kgf/cm}^2)$	49.0 ^{*1}	56.8	0.86	52.0 ^{*1}	65.2	0.80
Shear Yielding Strain $\gamma_y (\times 10^{-3})$	4.13 ^{*2}	4.43	0.93	3.51 ^{*2}	4.48	0.76

*1,*2 show maximum stress and maximum strain

T.V:Test value

C.V:Calculated value

Formulas $KG = E_0/2(1 + \gamma)$

$\tau_{cr} = \sqrt{c\sigma_B(\sqrt{c\sigma_B - \gamma\sigma_0})}$

$\tau_y = 1/2[(xP_w s\sigma_y - x\sigma_0) + (\gamma P_w s\sigma_y - \gamma\sigma_0)]$

$\tau_u = 3.5\sqrt{c\sigma_B}$

$\gamma_y = 2(E_0 + P_w \cdot E_s) s\epsilon_y / E_0 + 2(x\sigma_0 + \gamma\sigma_0) / E_0$

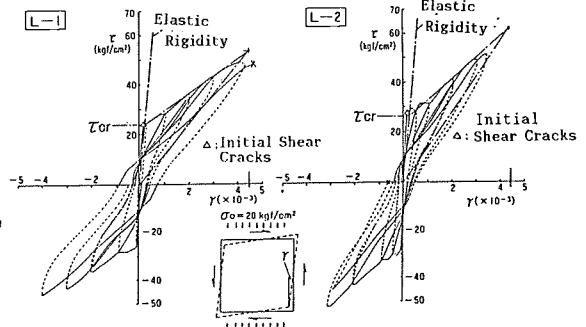


Fig. 3 Relationship of Shear Stress and Shear Strain

loading set-up of the test. The loading procedure was determined as follows: for the first and second cycles, loading was controlled to enable observation of behavior near point of initial shear cracking, and from the third cycle deformation was controlled by the deformation angle. Finally, the maximum load carrying capacity was confirmed at peak load by increasing the lateral loading.

Test results are shown in Table 5 and in Figs.6-8. The hysteresis loops were similar in shape for all specimens regardless of concrete strength, but after a rotation angle of $R=4 \times 10^{-3}$ rad. the capacity of the specimens using $F_c=360 \text{ kgf/cm}^2$ concrete increased remarkably. Fig.7 compares the envelope curves showing shear deformation for each specimen after standardizing the averaged shear stress using the square root $\sqrt{c\sigma_B}$ of the concrete strength. The envelope curve of each specimen with $M/QD=0.5$ has similar characteristics up to a shear strain $\gamma=3 \times 10^{-3}$. The maximum capacity of the specimen using $F_c=240 \text{ kgf/cm}^2$ strength concrete was observed at $\gamma=5.5 \times 10^{-3}$, while the maximum capacity of the specimen using $F_c=360 \text{ kgf/cm}^2$ strength concrete increased to $\gamma=8 \times 10^{-3}$. When the specimens with a shear span ratio of $M/QD=1.0$ are compared, all three specimens showed almost the same behavior and the deformation at their maximum capacity was $\gamma=5 \times 10^{-3}$. Table 5 shows a comparison between the test results and the calculated values. The initial rigidity of the specimens with $M/QD=0.5$ in the test was 20% to 30% less than the calculated value, but that of the specimen with $M/QD=1.0$ agreed with the calculated value. Fig.8 shows a

Table 4 List of Specimen

F_c (kgf/cm ²)	t (cm)	M/QD	0.5		1.0	
			10	20	10	20
240	15	0.5	1.06 ($\phi 90$)	W-15-1		W-15-2
			0.90 ($\phi 130$)	W-12-2		
360	12	0.5	1.32 ($\phi 90$)	W-12-4	W-12-1	W-12-7
			1.69 ($\phi 70$)	W-12-3		
420		1.0	1.32 ($\phi 90$)	W-12-5		

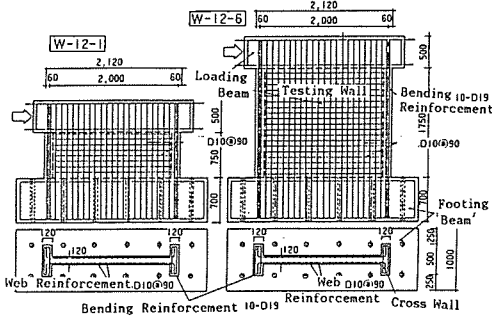


Fig. 4 Details of Bending Shear Tests Specimen

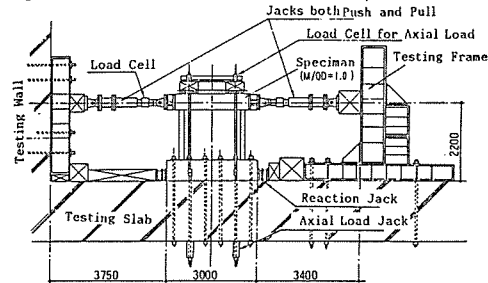


Fig. 5 Loading Set-up Bending Shear Tests

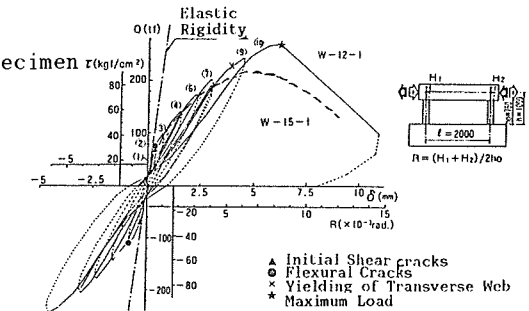


Fig. 6 Relationship of Lateral Load and Deflection

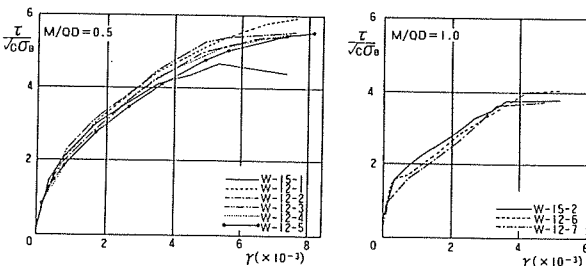


Fig. 7 Relationship of $\tau/\sqrt{c\sigma_B}$ and γ

Hirosawa's Formula

$$Q_u = \left(\frac{0.058 \cdot P_l \cdot \sigma_c^{0.75} (c\sigma_B + 180)}{M/QD + 0.12} + 0.5(P_w \cdot \sigma_y + 2.7\sqrt{P_w \cdot \sigma_y}) + 0.1\sigma_0 \right) \cdot l \cdot t$$

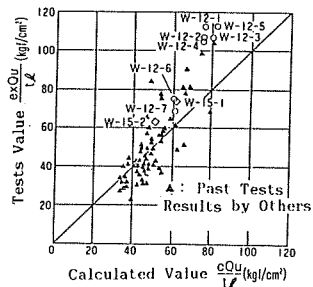


Fig. 8 Comparison of Tests Results and Calculated Value by Hirosawa's Formula

comparison between test results and calculated values. The test results were safely above the calculated values, showing a trend similar to that of previous test results obtained by other researchers, which are also plotted in the figure.

(3) THREE DIMENSIONAL MODEL BENDING SHEAR TEST

This test was designed to measure the restoring property of three dimensional models which were subjected to the bending shear test, both for the box type wall and the cylinder type wall. The three box specimens had the same wall length and thickness as the specimen with M/QD=0.5 in test (2), and were built with concretes of differing strengths. The web reinforcements, 10mm diameter, were arranged 90mm mesh in two layers 40mm apart. The ratios of web reinforcement differed according to the wall thicknesses of the specimens, being Pw=1.06% and Pw=1.32%. There was only one cylinder type specimen, which used Fc=360kgf/cm² strength concrete and had a wall thickness of 12cm, a web reinforcement ratio of Pw=1.2%, and a shear span ratio of M/QD=0.67. Table 6 shows a list of specimens and Table 7 shows the mechanical properties of the materials. Fig.9 shows details of the web reinforcement of the three dimensional test specimens.

Table 5 Comparison of Tests Results and Calculated Value

Specimen	Concrete Strength (kg/cm ²)	Initial Stiffness (t/cm)		Shear Cracks Load (t)		Ultimate Shear Capacity (t)		
		T.V	C.V	T.V	C.V *1	T.V	C.V *2	C.V *3
		W-15-1	253	2,890	3,300 (0.88)	79	72 (1.09)	223
W-12-1	359	2,530	3,160 (0.80)	68	65 (1.04)	271	186 (1.46)	224 (1.21)
W-12-2	389	2,930	3,270 (0.90)	60	67 (0.89)	256	185 (1.38)	209 (1.22)
W-12-3	365	2,690	3,200 (0.84)	73	66 (1.11)	256	194 (1.32)	246 (1.04)
W-12-4	365	2,360	3,190 (0.74)	57	56 (1.09)	253	184 (1.38)	224 (1.13)
W-12-5	412	2,300	3,380 (0.68)	48	69 (0.70)	272	199 (1.37)	238 (1.14)
W-15-2	264	1,230	1,040 (1.22)	80	73 (1.10)	155	155 (1.19)	166 (1.11)
W-12-6	338	1,090	970 (1.13)	73	64 (1.14)	179	148 (1.21)	161 (1.11)
W-12-7	346	830	980 (0.85)	55	55 (1.01)	169	147 (1.14)	159 (1.06)

* 1 $Q_{cr} = \sqrt{k\sigma_c(V\sigma_c + \sigma_o)} \cdot t \cdot l$ (Ratio of test value dividing calculated value)

* 2 $Q_u = \left[\frac{0.068 \cdot P_t \cdot l^2 (\sigma_c + 180)}{\sqrt{M/QD + 0.12}} + 2.7 \sqrt{P_w \cdot \sigma_y + 0.1 \sigma_o} \right] b \cdot t$

* 3 $Q_u = \left[\frac{0.068 \cdot P_t \cdot l^2 (\sigma_c + 180)}{M/QD + 0.12} + 0.5 (P_w \cdot \sigma_y + 2.7 \sqrt{P_w \cdot \sigma_y} + 0.1 \sigma_o) \right] t \cdot l$

Observing the load deflection curves shown in Fig.10, those of the specimen made of Fc=360kgf/cm² strength concrete were of a similar shape to that of the specimen made of Fc=240kgf/cm² strength concrete. Fig.11 shows a comparison between the averaged shear stress and the rotation angle. Though all specimens displayed the same behavior up to shear cracks load (up to 30kgf/cm² {2.9MPa}), that which accompanied the appearance of), the capacities of both the Fc=360kgf/cm² and Fc=420kgf/cm² specimens increased, as the lateral load became larger. Comparing maximum capacities, that of the Fc=360kgf/cm² specimen was $\tau=108\text{kgf/cm}^2$ {11MPa}(about 11% larger). The deformations of the Fc=240kgf/cm² and Fc=360kgf/cm² specimens at maximum capacities were about $R=8 \times 10^{-3}$ rad., but that of the Fc=420kgf/cm² specimen was about $R=10 \times 10^{-3}$ rad. Which was larger than that of the other specimens. Both the rigidity and the maximum capacity of the cylinder type specimen were less than those of the box type specimens, as its shape and shear span ratio were different. The shear deformation, and then the final crashing of each specimen were proved to be the compressive shear failure on the web concrete.

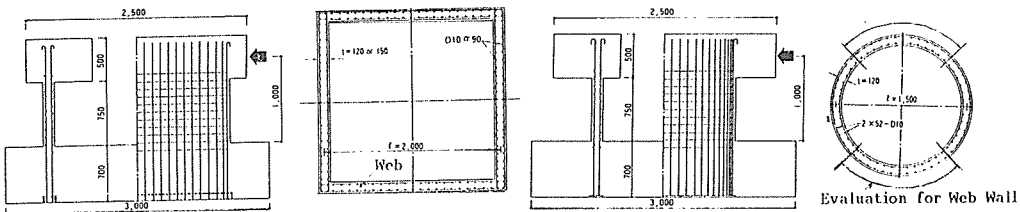


Fig. 9 Details of Three Dimensional Tests Specimen

AW=0.5A
AW: Total Area of Wall
A : Web Area

Table 6 List of Specimen

Type	Speciman	Concrete Strength (kg/cm ²)	Wall Thickness (cm)	Ratio. Pw (%)	Shear Span Ratio	Axial Stress σ_a (kg/cm ²)
Box Type	B-240	240	15	1.06	0.5	20
	B-360	360	12	1.32	0.5	20
	B-420	420	12	1.32	0.5	20
Cylinder	S-360	360	12	1.32	0.67	20

Table 7 Mechanical Properties of Concrete

Speciman	Concrete			Web Reinforcement	
	Compressive Strength (kg/cm ²)	Young's Modulus ($\times 10^5$ kg/cm ²)	Tensile Strength (kg/cm ²)	D10, SD35	
B-240	292	2.41	25	Yielding Stress	3760 kg/cm ²
B-360	378	2.67	31	Yielding Strain	2177×10^{-6}
B-420	440	3.01	32	Tensile Strength	5360 kg/cm ²
S-360	380	2.68	31	Young's Modulus	1.74×10^6 kg/cm ²

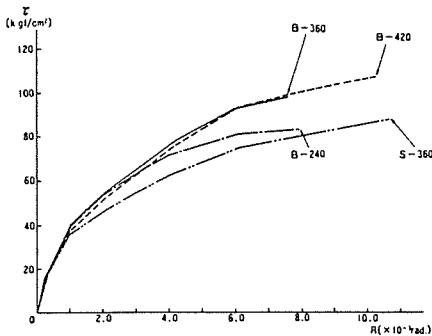
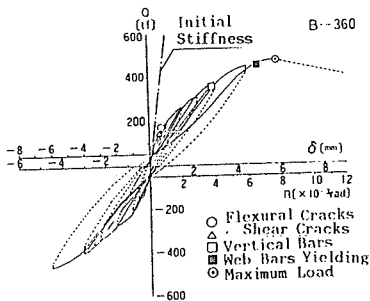


Fig.11 Comparison of Averaged Shear Stress and Rotation Angle

Table 8 Comparison of Tests Results and Calculated Value

Speciman		B-240	B-360	B-420	S-360
Initial Stiffness (t/cm)	T.V	7120	5590	4120	2600
	C.V *1	7710(0.92)	6860(0.81)	7760(0.53)	3350(0.78)
Shear Cracks load (t)	T.V	160	130	121	70
	C.V *2	151(1.06)	133(0.98)	141(0.88)	78(0.87)
Ultimate Shear Capacity (t)	T.V	504	474	519	248
	C.V *3	340(1.48)	327(1.45)	351(1.48)	189(1.31)
	C.V *4	376(1.34)	350(1.35)	365(1.42)	201(1.23)

(): T.V/C.V *1: Beam Theory *2-4: See Fig.16
 T.V: Test value C.V: Calculated value

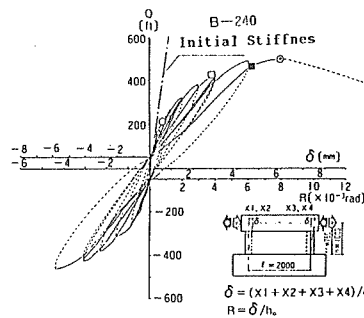


Fig.10 Load-Deflection Curves

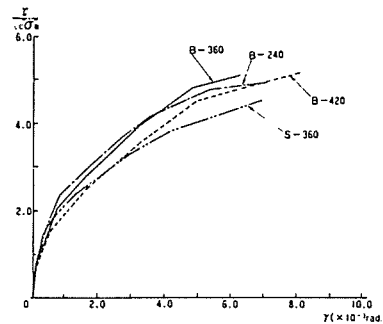


Fig.12 Comparison of $\tau/\sqrt{\sigma_B}$ and γ

CONCLUSION

- Observing the relationship between the standardized values of the averaged shear stress, shear strain, and deformation angle, in Fig.13 and Fig.14, all tests confirmed that shear walls using the higher strength concrete $F_c=360\text{kgf/cm}^2$ could be considered to have structural properties equal to those of shear walls using concrete of usual strength, although wall thickness of the former was reduced to 80% of the usual wall thickness.
- The relationship between the ratios of test results to estimated values and concrete strength is shown in Fig.15. The ratios were appeared to increase in accordance with the concrete strength, and therefore the test results were higher within 1.14 and 1.48 times than the calculated values. Estimations of ultimate shear capacity calculated by Hirosawa's modified formula and by Yoshizaki's formula showed in Fig.16 noted *3, were not remarkably different from each other.

c. A comparison of the τ - γ curve obtained from the test results of specimen B-360 and the skeleton curve produced by calculations employing conventional formulas is shown in Fig.16. The two curves appear rough correspondence, and we could recognize the aseismic safety of Nuclear Power Plants using higher strength concrete. But the suitable evaluation of the maximum deformation and capacity remains problematic.

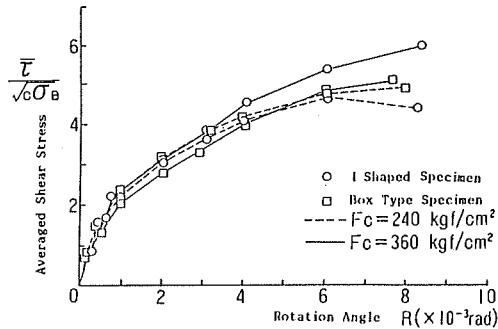
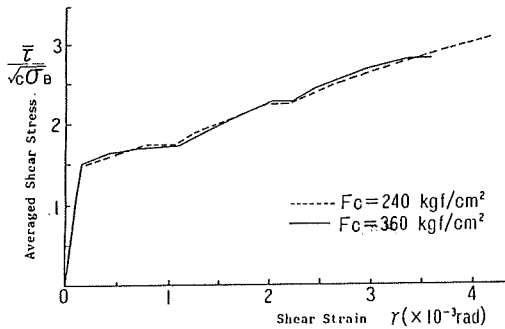


Fig.13 Effect of Wall Thickness Reducing in Large Panel Tests

Fig.14 Effect of Wall Thickness Reducing in I Shaped Shear Wall Tests and Three Dimensional Model Tests

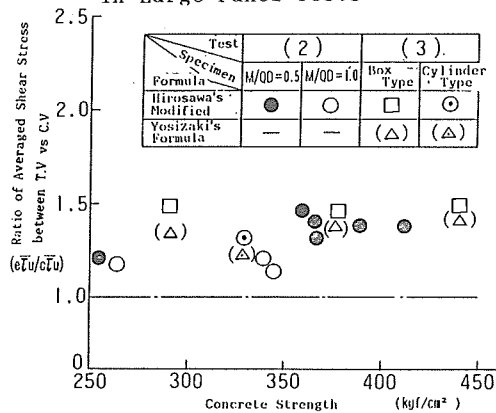


Fig.15 Comparison of Tests Results and Calculated Value for Ultimate Shear Strength

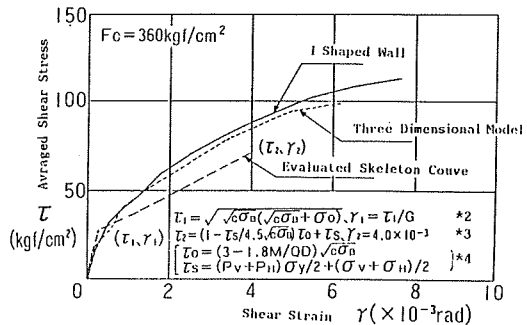


Fig.16 Evaluation of Shear Skeleton Curves on Bending Shear Tests

ACKNOWLEDGMENTS

This study was carried out by Tokyo Electric Power Company, which was a manager, Tohoku Electric Power Company, Chubu Electric Power Company, Hokuriku Electric Power Company, Chugoku Electric Power Company, Japan Atomic Power Company and Kajima corporation, all of Japan. We express our heartfelt thanks to Dr. K. Ogura, Dr. H Aoyama, Dr. K. Shiroyama, and Dr. H. Akiyama for their consulting, and to our colleagues for their assistance.

REFERENCE

- (1)Architectural Institute of Japan "The potential seismic load carrying capacities and the deformation capacity on the aseismic structural design of building"1981,June.
- (2)A. Yano, M. Kanechika, and K. Okamoto, et al. "Experimental Study of Shear Wall using High Strength Concrete (No.1-No.4)" SUMMARIES OF TECHNICAL PAPERS OF ANNUAL MEETING ARCHITECTURAL INSTITUTE OF JAPAN 1986. STRUCTURE II